

Solution Processable Si/Ge Heterostructure NWs Enabling Anode Mass Reduction for Practical Full-cell Li-ion Batteries

Temilade Esther Adegoke ^{§a}, Syed Abdul Ahad ^{§a}, Ursel Bangert ^b, Hugh Geaney ^{*a}, Kevin M. Ryan ^{*a}

^aDepartment of Chemical Sciences and Bernal Institute, University of Limerick, Limerick, V94 T9PX Ireland.

E-mail: kevin.m.ryan@ul.ie, hugh.geaney@ul.ie

^bDepartment of Physics and Bernal Institute, University of Limerick, Limerick, V94 T9PX Ireland.

§ These authors contributed equally to the work

SUPPLEMENTARY MATERIALS

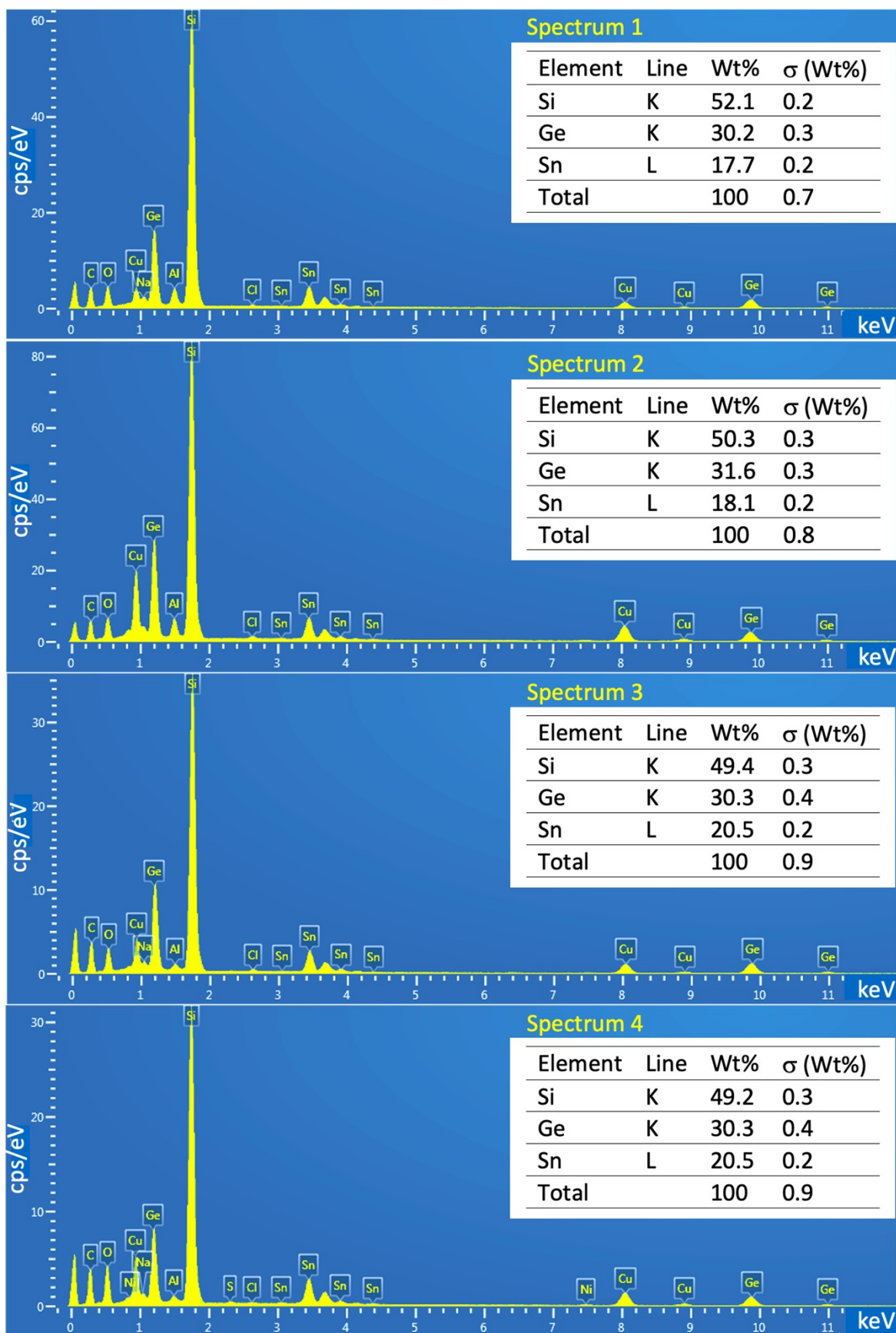


Figure S1. Quantitative EDX estimation of the % weight of Si, Ge and Sn from multiple areas of the anode. The mean value was obtained (Sn:Si:Ge weight % ratio is: 18:50:32).

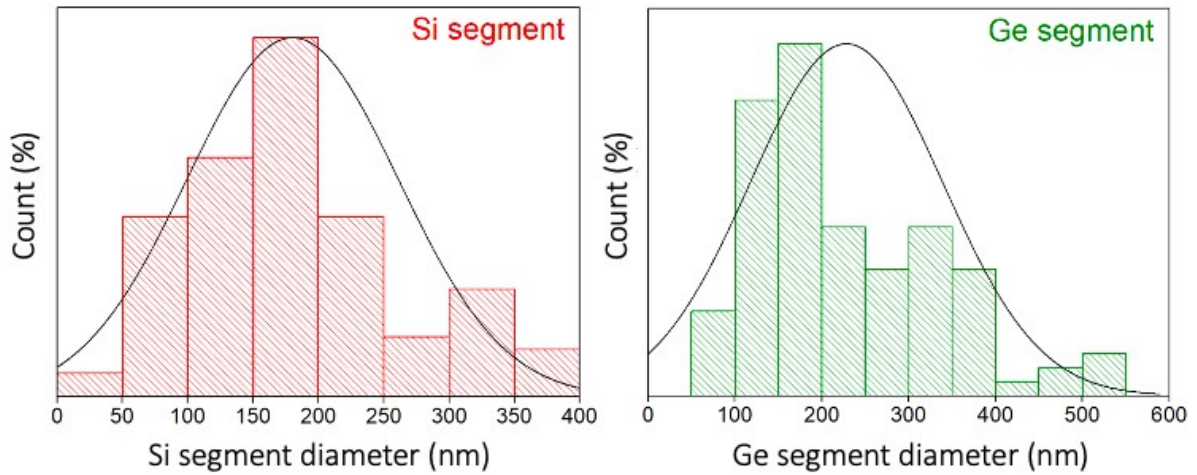


Figure S2. Histograms representing NW diameter distribution of Si and Ge segment in hSG NWs. Each distribution was obtained by direct counting method, measuring the diameters for 200 NWs from SEM images.

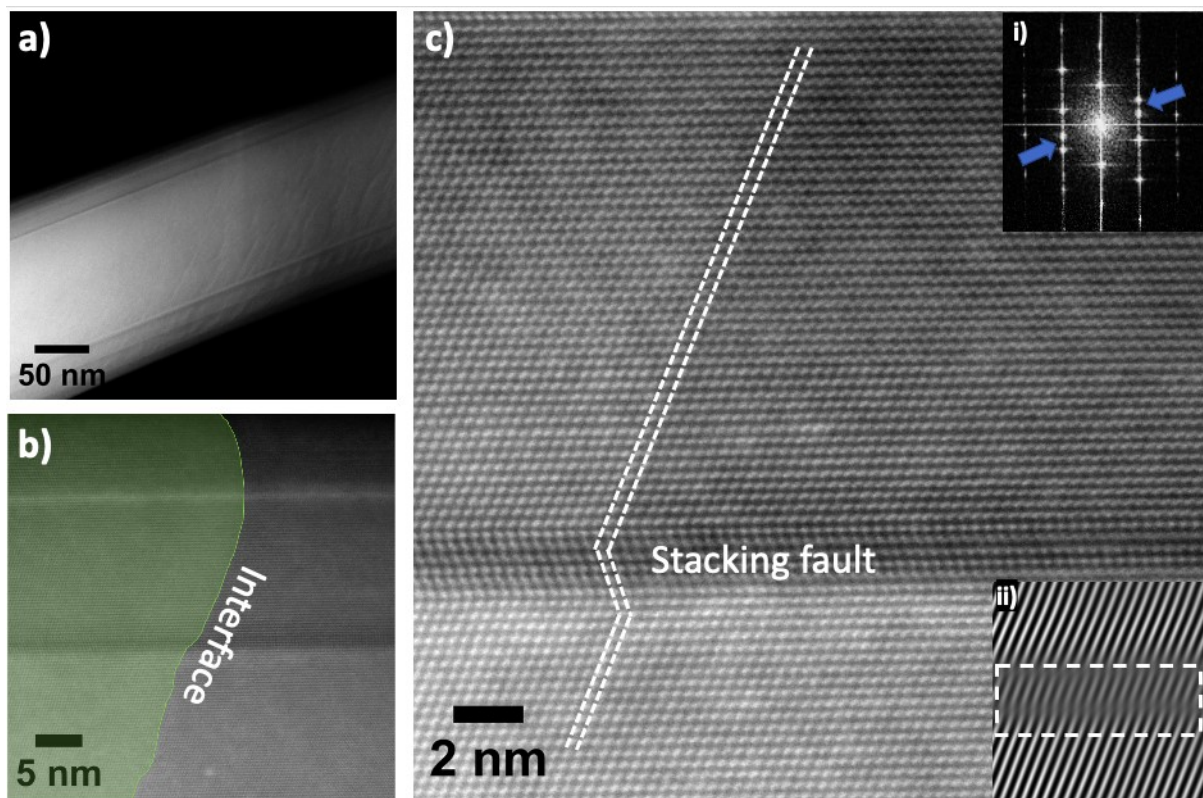


Figure S3. (a) HAADF-STEM image of hSG NW viewed from $\langle 110 \rangle$ orientation. (b) High-resolution image, heterointerface highlighted by the green overlay, showing defect across the Si-Ge segment. (c) Atomic-resolution image of the heterointerface indicating SF marked by the white dashed lines. Insets are (i) FFT spots and (ii) IFFT image corresponding to the regions of SF.

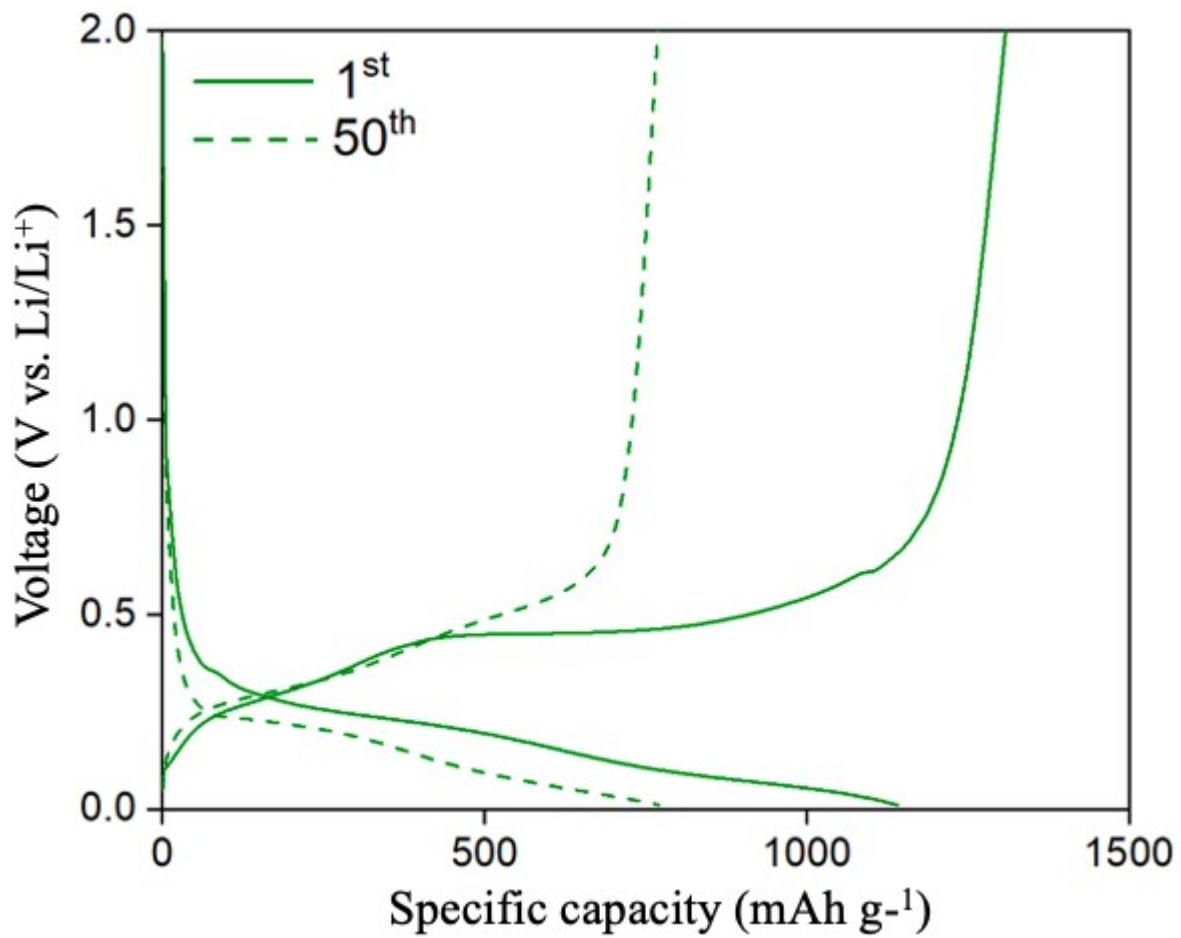


Figure S4. Voltage - Specific capacity profile of Si NWs (slurry) for 1st and 50th cycle at 0.2 C.

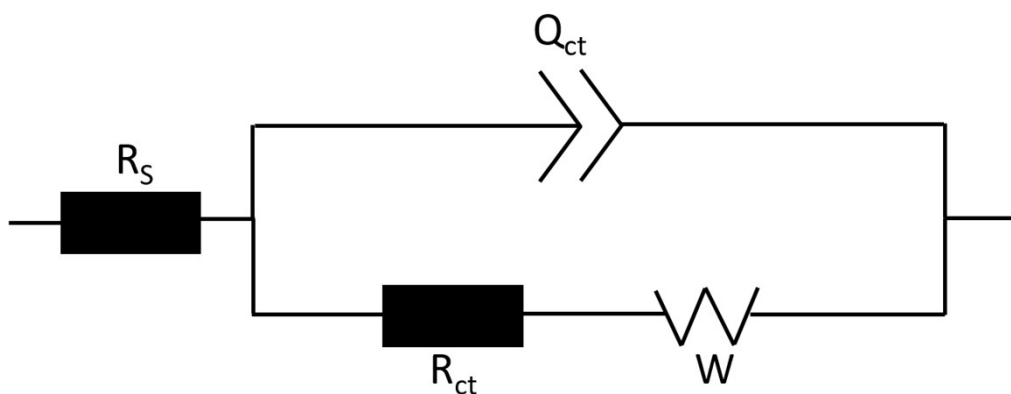


Figure S5. Fitting circuit used for EIS analysis.

	R_s (ohm)	R_{CT} (ohm)
1 st cyc	19.29	47.98
50 th cyc	19.96	5.17

Table S1. Tabulation of R_s and R_{ct} values of hSG NWs after 1st and 50th cycle.

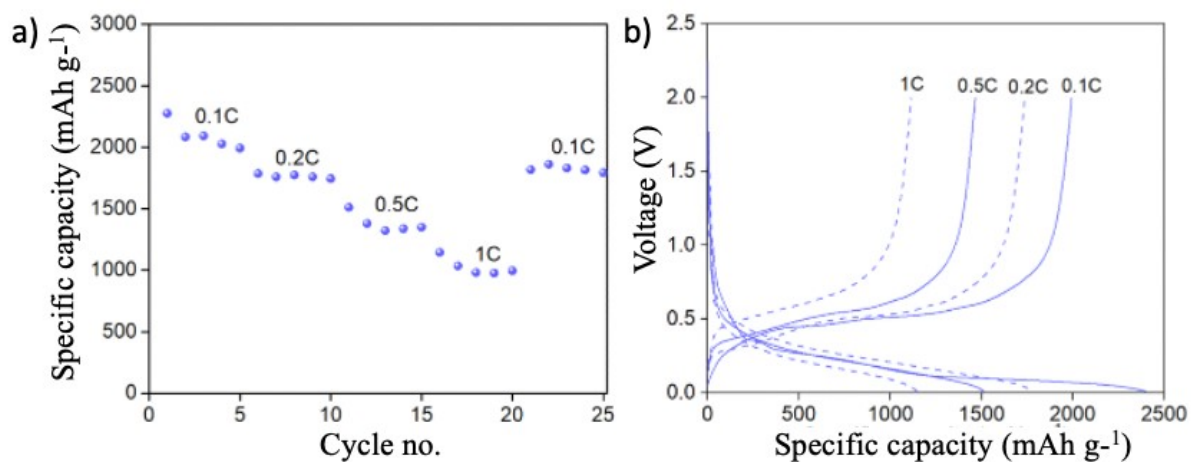


Figure S6. (a) Rate capability test and (b) corresponding voltage – specific capacity plot of hSG NWs at various C-rates.

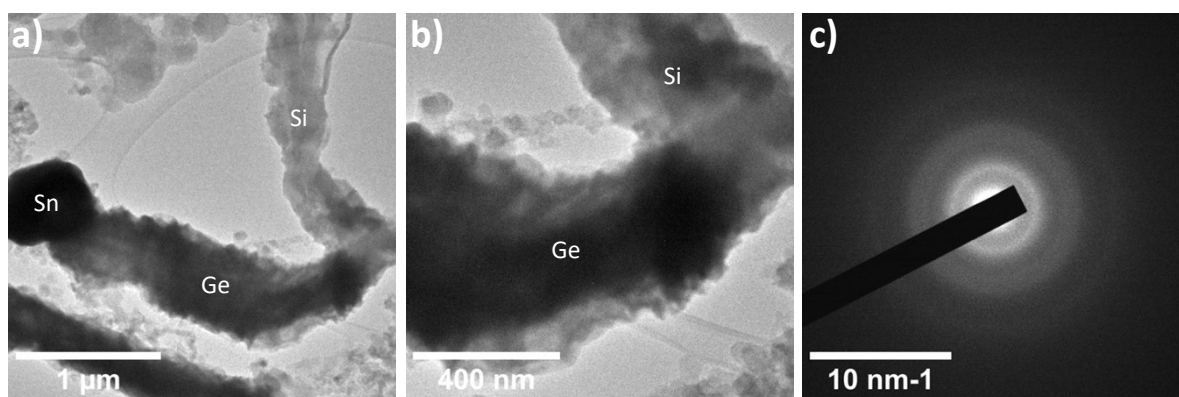


Figure S7. TEM analysis of the hSG anode at the 5th cycle (a) low magnification TEM image of the Sn, Si and Ge segments. (b) high magnification of Si and Ge segments. (c) Diffraction pattern of b with both segments now amorphous.

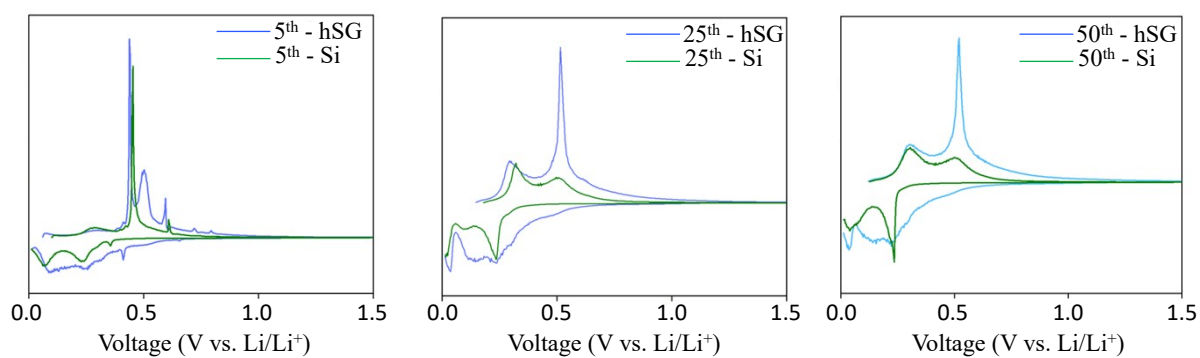


Figure S8. Comparison of dQ/dV curve of hSG and Si NWs at 5th, 25th and 50th cycle (at 0.2 C).

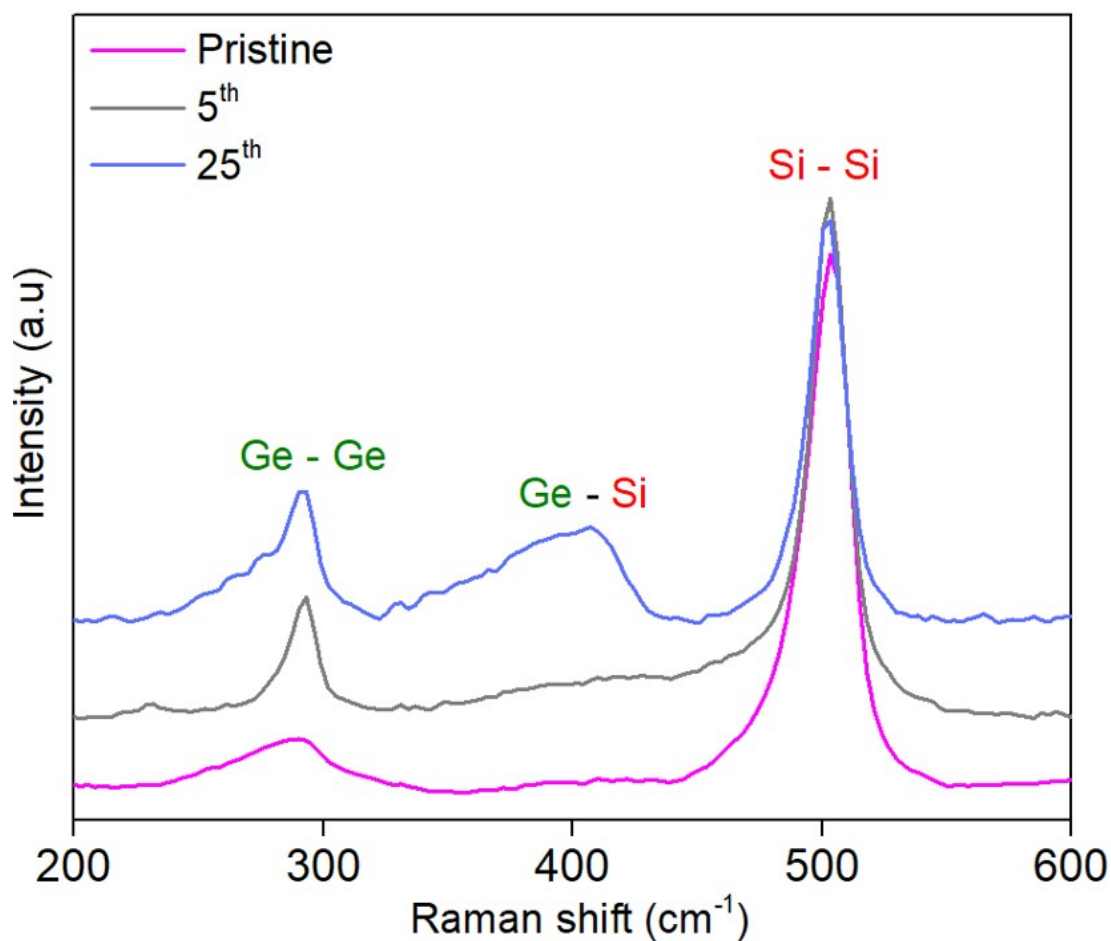


Figure S9. Raman spectroscopy analysis of hSG NWs before cycling (pristine), after 5th and 25th cycle.

Anode material	Active mass (mg cm ⁻²)	Total anode mass (mg cm ⁻²)	Anode mass reduction (%)
Graphite	4.56	5.07	50.7 %
hSG	1.5	2.5	

Table S2. Anode mass reduction calculation of hSG vs. standard graphite anode using P/N ratio of 1.18. The total anode mass consists of active material, conductive agent and binder weight as well. For graphite anode total mass calculation, a standard slurry composition of 90 % graphite, 5 % conductive agent and 5 % binder was used. The theoretical capacity of graphite used was 372 mAh g⁻¹.

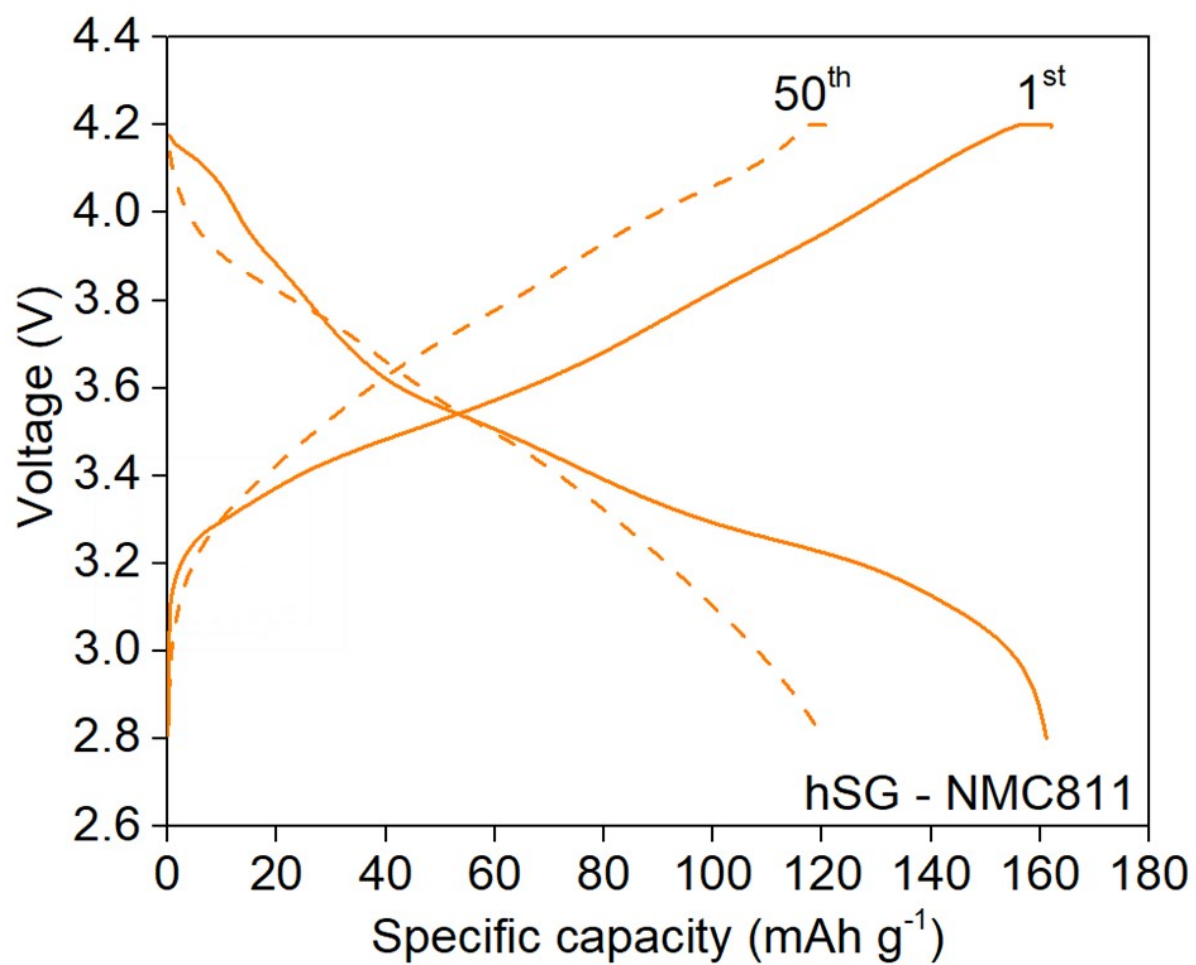


Figure S10. Voltage – specific capacity plot of hSG – NMC811 cell after 1st and 50th cycled at 0.2 C.